

**TITLE PAGE**

**Arsenite Inhibition of CYP1A1 Induction by TCDD is Independent of Cell Cycle Arrest**

by

Jessica A. Bonzo, Shujuan Chen, Alema Galijatovic<sup>†</sup>, and Robert H. Tukey.

Laboratory of Environmental Toxicology

Departments of Pharmacology, Chemistry & Biochemistry

University of California, San Diego

La Jolla, CA, 92093

## RUNNING TITLE PAGE

Title: Arsenite and CYP1A1 induction.

Address Correspondence to:

Robert H. Tukey, Ph.D.

University of California, San Diego

Leichtag Biomedical Research Building

Room 211

La Jolla, CA, 92093-0722

Tel: 858-822-0288

Email: [rtukey@ucsd.edu](mailto:rtukey@ucsd.edu)

Number of text pages: 33

Tables: None

Figures: Six

References: 37

Abstract: 242 words

Introduction: 729 words

Discussion: 897 words

## Abbreviations

As<sup>3+</sup>, arsenite; CYP1A1, cytochrome P450 1A1; HepG2, human hepatocarcinoma cell line; TCDD, 2,3,7,8-tetrachlorodibenzo-*p*-dioxin; EROD, ethoxyresorufin-*o*-deethylase; RT-PCR, reverse

transcriptase-polymerase chain reaction; Ah, arylhydrocarbon; XRE, xenobiotic responsive element; PARP-1, poly(ADP-ribose)polymerase I; B[a]P, benzo[a]pyrene; ATM, ataxia telangiectasia-mutated; PAH, polycyclic aromatic hydrocarbon; Arnt, arylhydrocarbon receptor nuclear translocator; hepa1c1c7, mouse liver carcinoma cell line; MTT, 3-(4-,5-dimethylthiazol-2-yl)-2,5-diphenyl tetrazoliumbromide; DMSO, dimethyl sulfoxide; DPBS, Dulbecco's phosphate buffered saline; BPDE-2, B[a]p-*r*-7,*t*-8-dihydrodiol-*t*-9,10-epoxide; TV101L, HepG2 cells stably transfected with hCYP1A1 promoter luciferase construct; HO-1, heme oxygenase 1; NQO1, NAD(P)H:quinone oxidoreductase; DMEM, Dulbecco's Modification of Eagle's Medium; G418, geneticin; PI, propidium iodide; FBS, Fetal Bovine Serum; DEPC, diethyl pyrocarbonate; NADPH, Nicotinamide adenine dinucleotide phosphate, reduced; EMSA, electrophoretic mobility shift assay; IKK $\beta$ , I $\kappa$ B kinase $\beta$ ; CYP, cytochrome P450

## Abstract

We show here that arsenite ( $\text{As}^{3+}$ ) elicits multiple effects on gene control, such as the interruption of cell cycle control by initiating G2/M arrest as well as inhibiting the Ah receptor mediated TCDD inducible expression of CYP1A1. This raises the question as to whether  $\text{As}^{3+}$  is selectively inhibiting TCDD induction of CYP1A1 independent of cell cycle control.  $\text{As}^{3+}$  stimulated a concentration-dependent increase in G2/M phase arrest that was detected at 12.5  $\mu\text{M}$   $\text{As}^{3+}$ . However, cotreatment of HepG2 cells with TCDD and concentrations of  $\text{As}^{3+}$  as low as 0.5  $\mu\text{M}$  stimulated a pronounced decrease in the induction of CYP1A1 dependent EROD activity and protein, indicating that the inhibition of CYP1A1 induction by  $\text{As}^{3+}$  was considerably more sensitive than  $\text{As}^{3+}$  initiated cell cycle arrest. Low concentrations of  $\text{As}^{3+}$  also initiate a dose dependent reduction in TCDD induced mouse Cyp1a1 as well as human CYP1A1 in primary hepatocytes cultured from transgenic *CYP1A1*<sup>+/−</sup> mice. Since primary hepatocytes in culture are quiescent, these results indicate that the actions of  $\text{As}^{3+}$  on TCDD initiated induction of CYP1A1 are independent of cell cycle control.  $\text{As}^{3+}$  does not impact on Ah receptor function as evaluated by nuclear transport and binding to XRE sequences, but does reduce TCDD induced CYP1A1 mRNA, a property that is concordant with RNA polymerase II association to the gene and the reduction in transcriptional heteronuclear RNA. We conclude from these studies that interruption of *CYP1A1* induced transcription by  $\text{As}^{3+}$  is not dependent upon cell cycle arrest.

## Introduction

Inorganic arsenic (arsenite,  $\text{As}^{3+}$ ) is an environmental contaminant released from a number of anthropogenic sources and results in  $\text{As}^{3+}$  sequestration in ground water which is often consumed as drinking water. Epidemiological studies indicate that chronic exposure is linked to vascular diseases associated with the cardiovascular and cerebrovascular systems, as well as the peripheral vasculature that leads to black foot disease (Tchounwou *et al.*, 2003; Chiou *et al.*, 1997; Lee *et al.*, 2003). In humans,  $\text{As}^{3+}$  exposure has also been thought to be a human carcinogen since epidemiological studies have linked  $\text{As}^{3+}$  exposure to skin, lung, liver, bladder, prostate and kidney cancers (Tchounwou *et al.*, 2003; Smith *et al.*, 1992). However, exposure of laboratory animals to  $\text{As}^{3+}$  has failed to produce organ specific cancers. This would indicate that cancers in humans linked to  $\text{As}^{3+}$  exposure may be associated with additional waterborne contaminants that work in concert to predispose humans to a carcinogenic episode. While the relationship between  $\text{As}^{3+}$  exposure and other environmental toxicants associated with a carcinogenic episode is not known, it would appear that the actions of  $\text{As}^{3+}$  on cellular functions influence the biological actions of other environmental toxicants.

$\text{As}^{3+}$  has been shown to alter cell cycle control, causing G1 and/or G2/M phase arrest with subsequent programmed cell death (Yih and Lee, 2000; Park *et al.*, 2000). Evidence suggests that the phase arrest is induced by DNA damage. Telomere shortening and chromosome end-to-end fusions (Liu *et al.*, 2003), oxidative DNA base modifications (Schwerdtle *et al.*, 2003), and DNA strand breaks (Yih and Lee, 2000) indicate that small amounts of direct DNA damage can be caused by low concentrations of  $\text{As}^{3+}$ . If DNA damage is not repaired, p53 induces cell arrest which eventually leads to apoptosis. It has been shown that p53 expression and ATM-dependent activation associated with G1 and G2/M arrest and apoptosis is up regulated upon  $\text{As}^{3+}$  treatment (Yih and

Lee, 2000;Filippova and Duerksen-Hughes, 2003;Park *et al.*, 2000). Thus, modulations in cell cycle control by  $As^{3+}$  exposure may impact on the expression of other cellular components.

The expression of CYP1A1 is dependent on the induction and activation of the arylhydrocarbon (Ah) receptor. Cell cycle control has been shown to influence CYP1A1 expression through mechanisms involving the Ah receptor and other independent pathways. When murine hepalc1c7 cells were treated with microtubule disrupters known to cause G2/M phase arrest, induction patterns of CYP1A1 following exposure to TCDD were dramatically reduced (Santini *et al.*, 2001). In addition, this arrest appeared to not disrupt Ah receptor functionality. Analysis of Ah receptor and Arnt proteins revealed no decrease in protein levels, nor was nuclear translocation of the activated Ah receptor impaired in G2/M arrested cells. Further implication that cell cycle control has an effect on CYP1A1 expression comes from data demonstrating that pRb binds to the Ah receptor and is necessary for maximal CYP1A1 induction by TCDD in G1 phase (Elferink *et al.*, 2001).

While  $As^{3+}$  can initiate cell cycle arrest, the levels of polycyclic aromatic hydrocarbon (PAH)-induced CYP1A1 are also inhibited when cells are exposed to  $As^{3+}$  (Vernhet *et al.*, 2003; Jacobs *et al.*, 1999). Since the Ah receptor is activated in response to PAHs leading to transcriptional activation of *CYP1A1*, it has been suggested that  $As^{3+}$  mediates the down-regulation of CYP1A1 through modulation of Ah receptor function. Transcriptional assays using reporter genes containing repeats of the xenobiotic responsive element (XRE) have demonstrated slight inhibition of transcriptional activity, suggesting that  $As^{3+}$  inhibits CYP1A1 induction through a transcriptional based mechanism (Vernhet *et al.*, 2003). However, the cellular mechanism underlying inhibition of CYP1A1 induction by  $As^{3+}$  remains largely unknown.

In this study, we have examined the effects of  $\text{As}^{3+}$  on Ah receptor control and the impact on TCDD-induced CYP1A1 expression. Given the known effects of  $\text{As}^{3+}$  on cell cycle control and apoptosis, the role of  $\text{As}^{3+}$ -induced G2/M arrest on TCDD initiated induction of CYP1A1 in HepG2 cells was investigated. Using a range of  $\text{As}^{3+}$  concentrations from sub-cytotoxic to levels that cause cellular arrest and apoptosis, we show that inhibition of CYP1A1 induction occurs at concentrations of  $\text{As}^{3+}$  well below those which initiate cell cycle arrest and apoptosis. The effects of  $\text{As}^{3+}$  on human *CYP1A1* gene expression in primary hepatocytes from transgenic mice (Galijatovic *et al.*, 2004) coupled with analysis of polymerase II recruitment lead us to conclude that  $\text{As}^{3+}$  inhibits CYP1A1 expression by modifying transcription independent of cell cycle control.

## Experimental Procedures

**Materials.** TCDD was purchased from Wellington Laboratories Inc (Ontario, Canada) and dissolved in DMSO. Sodium arsenite and the horseradish peroxidase-conjugated secondary antibody were purchased from Sigma (St. Louis, MO). A mouse anti-human PARP-1 antibody was purchased from Pharmingen (San Diego, CA) and the mouse anti-human  $\beta$ -actin and anti-Pol II (sc-5943) were purchased from Santa Cruz Biotechnology, Inc (Santa Cruz, CA). Rabbit anti-human CYP1A1 was a generous gift from Dr. Fred Guengerich, Vanderbilt University. The anti-human Ah receptor and anti-human Arnt antibodies were a generous gift from Dr. Chistopher Bradfield and the anti-human UGT antibody was a generous gift of Dr. Wilbert H. Peters. All other chemicals and reagents were obtained through standard suppliers.

**Cell culture.** The human hepatocarcinoma cell line HepG2 (American Type Tissue Culture) and mouse liver hepatoma hepalc1c7 cells (a generous gift of Dr James Whitlock, Stanford University) were cultured in DMEM supplemented with 10% fetal bovine serum. TV101L cells were derived from HepG2 cells that stably express a *CYP1A1*-luciferase reporter gene (Postlind *et al.*, 1993). TV101L cells were cultured under the same conditions as above, except Geneticin (G418; Gibco Brl, Gaithersburg, MD) was added to 0.8 mg/ml.

Primary hepatocytes were isolated from 8-12 week old *CYP1A1*<sup>+/−</sup> mice (Galijatovic *et al.*, 2004). Mice were anesthetized by isoflurane inhalation. The portal vein was cannulated while the anterior vena cava was sectioned to allow flow-through from the liver. Perfusion of the liver was started with Hank's balanced salt solution (no Ca<sup>2+</sup> or Mg<sup>2+</sup>) containing 0.5 mM EGTA and 10 mM Hepes (pH 7.4) at a rate of 4 ml/min and continued for 4 minutes. The perfusate was then changed to Hank's balanced salt solution (with Ca<sup>2+</sup> and Mg<sup>2+</sup>) containing 10 mM Hepes (pH 7.4) and 0.2 mg/ml collagenase. The liver was gently teased apart while in a solution of DMEM medium

containing 10% FBS supplemented with penicillin/streptomycin. The cells were filtered through a 70  $\mu$ m cell strainer and washed twice by centrifugation at  $50 \times g$  for 5 min. The hepatocytes were cultured into 6-well collagen-coated tissue culture plates (BD Biocoat). Four hours after plating, the medium was replaced. Primary hepatocytes were then treated 48 h after seeding and collected at the appropriate times after treatment.

**Cell Viability Assay (MTT Assay).** Cell viability was measured by 3-(4-,5-dimethylthiazol-2-yl)-2,5-diphenyl tetrazoliumbromide (MTT) as previously described (Mosmann, 1983). After treatment with various chemicals for 18 hours, culture medium was replaced with serum-free medium containing 0.5 mg/ml MTT and cultures were incubated for an additional 3 hours. Assay medium was removed and 1 ml of isopropanol with 0.04% HCl was added. Absorbance values were determined at 570nm and 630nm. Results are displayed as percent of viable cells compared to TCDD-treated cells.

**Cell cycle analysis.** Approximately  $1 \times 10^6$  HepG2 cells were exposed to TCDD and  $As^{3+}$  for 18 hours and the cells were collected by trypsinization and pelleted at  $1,000 \times g$  for 5 min. Cells were washed twice with 1 X DPBS and resuspended in 50  $\mu$ l 1 X DPBS. Cells were fixed by the slow addition of 70% ethanol with constant vortexing to a volume of 5 ml. The cells were pelleted and resuspended in 800  $\mu$ l 1 X DPBS containing 3% fetal bovine serum. 100  $\mu$ l of PI solution (final concentration 50  $\mu$ g/ml PI) and 100  $\mu$ l boiled RNase A (final concentration 1mg/ml) was added and incubated at 37°C for 30 min. Approximately  $1 \times 10^4$  cells were acquired on a FACS Calibur flow cytometer and analyzed using the CELLQuest software.

**Preparation of cellular and microsomal protein.** Total cellular protein was obtained by lysing cells directly on the tissue culture plates in 25 mM Hepes, pH 7.5, 0.3 M NaCl, 1.5 mM MgCl<sub>2</sub>, 0.2 mM EDTA, 0.1% Triton X-100, 20 mM  $\alpha$ -glycerophosphate, 0.5 mM DTT, 1 mM sodium orthovanadate, 0.1  $\mu$ M okadaic acid, and 1 mM PMSF. The solubilized cell lysate was collected, centrifuged at 10,000 x g, and the supernatant collected.

Microsomal protein was obtained by scraping cells from the tissue culture plates in a suspension of 10 mM KH<sub>2</sub>PO<sub>4</sub>, 0.15 M KCl, 2 mM PMSF, 2 mg/ml aprotinin, 0.2 mg/ml benzamidine, 0.5 mg/ml leupeptin, and 1  $\mu$ g/ml pepstatin. The cells were disrupted on ice by ultrasonic disruption employing 5 repetitive 5 sec bursts, followed by centrifugation at 10,000 x g. Supernatants were collected and centrifuged at 105,000 x g for 1 hour in a Beckman TL100 table-top ultracentrifuge. Microsomal pellet was resuspended in 100  $\mu$ l of the phosphate buffer and stored at -70°C. All protein concentrations were determined by Bio-Rad analysis according to the manufacturer's instructions.

**Western blot analysis.** Western blots for detection of PARP-1 were performed using NuPAGE Bis-Tris gel electrophoresis units as outlined by the manufacturer (Invitrogen, Carlsbad, CA). A 20  $\mu$ g aliquot of total cellular protein was heated for 10 min in loading buffer and resolved on a 10% Bis-Tris gel under reducing conditions and protein was transferred to a nitrocellulose membrane using a semi-dry transfer system (Novex, Invitrogen). The membrane was blocked with 5% nonfat dry milk in Tris-buffered saline (0.01M Tris pH 8.0, 0.150M NaCl, and 0.05% Tween-20) overnight at 4°C. This was followed by incubation with an anti-human/mouse PARP-1 primary antibody in Tris-buffered saline for 1 hour at room temperature. Membranes were then washed and incubated for 1 hour with horseradish peroxidase-conjugated secondary antibody at room

temperature. The conjugated horseradish peroxidase was detected using ECL Plus Western blotting detection system (Amersham, Piscataway, NJ) and blots were exposed to X-ray film.

For detection of microsomal CYP1A1, 10 µg of microsomal protein was boiled in non-reducing loading buffer and added to Novex<sup>®</sup> 10% Tris-Glycine gels (Invitrogen) and electrophoresis carried out according to manufacturer's instructions. Membranes were then prepared as described above with the exception of the use of rabbit anti-human CYP1A1 primary antibody. For detection of CYP1A1 from primary hepatocytes, 20 µg of total cellular protein was used and blots performed as described for microsomal CYP1A1.

**Detection of ethoxyresorufin O-deethylase (EROD) activity.** EROD measurement was performed as previously described (Ciolino *et al.*, 1998). Approximately  $2.5 \times 10^5$  cells/well were plated in 6-well plates. Cells were exposed to TCDD and As<sup>3+</sup> for 18 hours and the media removed and replaced with DMEM containing 10% fetal bovine serum, 1.5 mM salicylamide, and 2.5 µM 7-ethoxyresorufin. After incubation for 30 min at 37°C, the media was removed and fluorescence measured with 530 nm excitation and 590 nm emission on a FluoroMax-2 (Yobin Yvon SPEX Instruments, S.A. Inc.). Resorufin standard curves were used to convert fluorescence to pmol of resorufin formed. Results were normalized to reaction time and cellular protein.

For determination of microsomal EROD activity, microsomes were collected and resuspended in 50 mM Tris-HCl, pH 7.5, 20% glycerol v/v, and 1 mM DTT. Reactions contained 20 µg protein and 8 µM 7-ethoxyresorufin and were initiated by the addition of 1 mM NADPH. After incubation for 30 min at 37°C, each reaction was stopped with the addition of cold methanol. Fluorescence was detected as described above.

**RNA Analysis for *CYP1A1* expression.** Total RNA was extracted from cells using TRIzol® (Invitrogen) according to manufacturer's protocol, and resuspended in DEPC treated water. Each preparation of RNA was treated with DNase using a DNA-free™ Kit (Ambion, Austin, TX). Levels of CYP1A1 mRNA and hnRNA were quantitated by real-time PCR. After oligo-dt-primed reverse transcription using 2 µg total RNA with Omniscript™ RT (Qiagen, Valencia, CA), the cDNA was amplified with forward (5'-TAG-ACA-CTG-ATC-TGG-CTG-CAG-3') and reverse (5'-GGG-AAG-GCT-CCA-TCA-GCA-TC-3') human CYP1A1 mRNA primers. Primers for human CYP1A1 hnRNA were previously published (Hestermann and Brown, 2003). For quantitation of human GAPDH, the forward (5'-GCT-GAG-ACA-CCA-TGG-GGA-AG-3', bases 93-113) and reverse (5'-CTT-CCC-GTT-CTC-AGC-CTT-GA-3', bases 282-301) primers were identified from the cDNA sequence (Accession number: AF261085). Each RNA was amplified in a 50 µl PCR reaction that contained 25 µl QuantiTect™ SYBR® Green PCR Master Mix (Qiagen), 100 nM each of forward and reverse primers, and 2 µl cDNA. The initial activation was proceeded at 95°C for 10 min followed by 40 cycles of amplification: 95°C 30 sec, 60°C 1 min, 72°C 45 sec. Amplification was followed by DNA melt at 95°C for 1 min and a 41 cycle dissociation curve starting at 55°C and ramping 1°C every 30 sec. The MX4000 Multiplex QPCR (Stratagene, La Jolla, CA) was programmed to take 3 fluorescence data points at the end point of each annealing plateau. All PCR reactions were performed in triplicates. CYP1A1 Ct values were normalized to GAPDH Ct values ( $\Delta Ct$ ). CYP1A1 cDNA and hnRNA was expressed as induction fold of vehicle treated cells using the equation:  $\text{ratio} = 2^{-(\Delta Ct_{\text{Sample}} - \Delta Ct_{\text{Vehicle}})}$  (Pfaffl, 2001). TCDD treated samples were set to maximal induction and all other treatments are expressed as a percent of TCDD induction of CYP1A1 mRNA.

**Nuclear and cytosolic protein preparation.** Nuclear protein was prepared as previously described (Chen and Tukey, 1996), and all procedures were performed at 4°C. After treatment, the tissue culture plates were washed twice with ice cold 10 mM HEPES. Cells were collected by scraping into MDH buffer (3 mM MgCl<sub>2</sub>, 25 mM HEPES, 1 mM DTT, 0.2 mM PMSF, 10 µg/ml aprotinin, and 10 µg/ml leupeptin) and homogenized with a Dounce homogenizer. The homogenate was centrifuged at 2500 x g for 5 min and the resulting nuclear pellet resuspended and washed three times with MDHK buffer (3 mM MgCl<sub>2</sub>, 25 mM HEPES, 0.1 M KCl, 1 mM DTT, 0.2 mM PMSF, 10 µg/ml aprotinin and 10 µg/ml leupeptin). The nuclear fraction was resuspended in 100 µl HDK buffer (25 mM HEPES, 0.4 M KCl, 1 mM DTT, 0.2 mM PMSF, 10 µg/ml aprotinin and 10 µg/ml leupeptin), incubated for 30 min on ice, and centrifuged at 16,000 x g for 15 min. The resulting supernatant was transferred to ultracentrifuge tubes, adjusted to a final concentration of 10% glycerol, and centrifuged at 105,000 x g for 1 h. Each nuclear protein aliquot was stored at -70°C.

Cytosols were prepared from untreated Hepa1c1c7 cells as described previously (Chen and Tukey, 1996). Briefly, cells washed in HEPES were collected by scraping in HED buffer (25 mM HEPES, pH 7.5, 1 mM EDTA, and 1 mM DTT). The cells were homogenized with a Dounce homogenizer and then diluted 1:1 with HED2G (25 mM HEPES, pH 7.5, 1 mM EDTA, 1 mM DTT, and 20% glycerol). The homogenate was centrifuged at 105,000 x g for 1 hour and the supernatant collected. Cytosolic Ah receptor was activated by incubation of cytosol with 20 nM TCDD for 24 hours at 4°C.

**Electrophoretic mobility shift assay (EMSA).** As previously described (Yueh *et al.*, 2003), nuclear or cytosolic extracts were incubated on ice for 15 min with 2.2 µg poly(dI-dC) and 1 µg salmon sperm DNA in HEDG buffer (25 mM HEPES pH 7.4, 1.5 mM EDTA, 10% glycerol, 1 mM DTT). A <sup>32</sup>P-labelled XRE oligonucleotide probe (5x10<sup>5</sup> cpm) was added and the reaction incubated

at room temperature for 15 min. Loading dye was added and the proteins resolved on a 6% non-denaturing polyacrylamide gel. Radioactively bound proteins were visualized by exposure to a phosphorimager plate and scanning with a Molecular Dynamics Storm 840 scanner.

**Luciferase activity assay.** Luciferase assays were performed as previously described (Chen and Tukey, 1996). TV101L cells were treated and lysed on plates in Lysis Buffer (1% Triton, 25 mM Tricin pH 7.8, 15 mM MgSO<sub>4</sub>, 4 mM EDTA, 1 mM DTT). Cell lysates were collected by centrifugation at 10,000 x g in a microcentrifuge for 10 min at 4°C. Supernatant (10 µl) was mixed with 300 µl reaction buffer (25 mM Tricine, 15 mM MgSO<sub>4</sub>, 4 mM EDTA, 15 mM KPO<sub>4</sub> pH 7.8, 1 mM DTT, 2 mM ATP). Reactions were started by the addition of 100 µl luciferin (0.3 mg/ml) and light output measured for 10 sec at 24°C using a Monolight 2001 luminometer (Analytical Luminescence Laboratory). Results were normalized by Bradford protein assay and expressed as fold induction of vehicle control.

**Chromatin Immunoprecipitation Assay.** Method was based on those previously published (Wei *et al.*, 2004; Hestermann and Brown, 2003). HepG2 cells were grown to confluency on 150 cm plates then treated for 1 hr with DMSO, TCDD, 0.5 µM As<sup>3+</sup> + TCDD, or 5 µM As<sup>3+</sup> + TCDD. Cells were cross-linked by addition of formaldehyde to 1% directly to culture media for 10min. Cross-linking was stopped by the addition of 125 mM glycine and cells were incubated at room temperature for 10 min with gentle rocking. Plates were washed with PBS and then cells collected by scraping in cold PBS. Cellular pellet was lysed (1% SDS, 5 mM EDTA, 50 mM Tris, pH 8, protease inhibitors) for 10 min on ice then sonicated 3 x 15 sec at 20 watts in 1 min intervals. The sample was cleared of cellular debris by centrifugation at 16,000 x g for 10 min at 4°C. One hundred µl aliquots were diluted to 1 ml in dilution buffer (1% Triton, 2 mM EDTA, 20 mM Tris,

pH 8, 150 mM NaCl, protease inhibitors) and precleared for 1 hr at 4°C with 50  $\mu$ l protein agarose A/G (Santa Cruz Biotechnology, Inc.) with 1  $\mu$ g/ $\mu$ l salmon sperm DNA. Aliquots were removed at this time for use as input control and processed along with pull-down DNA at reversal of cross-linking step. Precleared supernatants were then incubated overnight at 4°C on a rotating platform with 1  $\mu$ g  $\alpha$ -Pol II. Fifty  $\mu$ l protein agarose A/G plus salmon sperm DNA was added and incubated on rocking platform for 1 hr at 4°C. Beads were pelleted and washed 10 min each in following buffers (Buffer 1: 0.1% SDS, 2mM EDTA, 20 mM Tris, 150 mM NaCl; Buffer 2: 0.1% SDS, 2mM EDTA, 20 mM Tris, 500 mM NaCl; Buffer 3: 1% LiCl, 1% NP-40, 1% deoxycholate, 1 mM EDTA, 10 mM Tris). Pellets were washed twice in TE Buffer and then eluted in 100  $\mu$ l of 1% SDS, 0.1 M sodium bicarbonate, 0.2 M NaCl at 65°C overnight. Eluates were digested with proteinase K at 45°C for 1 hr and then purified using Qiagen spin columns. DNA was quantitated using a spectrophotometer. Equal amounts of pulled-down DNA as well as input controls were used for each quantitative real-time PCR reaction. Amplification of the proximal promoter was achieved using primers that span a 250 bp region that includes the transcription start site (forward 5' AGA-AAG-GGC-AAG-CCA-GAA-GT 3' and reverse 5' TCC-AAT-CCC-AGA-GAG-ACC-AG 3'). Results are displayed as raw C(t) values and representative of three independent experiments.

**Statistical analysis.** All experiments were performed in triplicate. Statistical analysis was performed where indicated using two-tailed T-test assuming unequal variances. Differences were determined to be significant if  $P \leq 0.05$ .

## Results

### ***Effect of As<sup>3+</sup> on apoptosis and cell cycle.***

As<sup>3+</sup> has been shown to interrupt normal cell function by interfering with cell cycle control and initiating apoptosis. To examine the impact of As<sup>3+</sup> on HepG2 cells, we treated cells with a range of As<sup>3+</sup> concentrations and measured cell viability by MTT analysis (Figure 1A) and apoptosis by detecting caspases activated PARP-1 cleavage (Figure 1B). Comparisons were made over a range of As<sup>3+</sup> concentrations that also included co-treatment with 10 nM TCDD. At concentrations of As<sup>3+</sup> ranging from 0.5  $\mu$ M to 25  $\mu$ M, no changes in cell viability or the initiation of apoptosis were noted. TCDD alone or in combination with As<sup>3+</sup> at these concentrations did not affect cell function. However, cell viability was reduced 30% in HepG2 cells treated with 50  $\mu$ M As<sup>3+</sup>, which correlated with a mild increase in caspases activated PARP-1 cleavage. When cell cycle status was evaluated, As<sup>3+</sup> treated HepG2 cells revealed an increase in G2/M cell cycle arrest at concentrations that exceeded 12.5  $\mu$ M (Figure 1C). Analysis of HepG2 cells treated with As<sup>3+</sup> alone was consistent with the results shown in Figure 2 indicating that the increase in G2/M arrest was attributed solely to the actions of As<sup>3+</sup>.

### ***As<sup>3+</sup> treatment blocks TCDD induction of CYP1A1.***

The co-treatment of HepG2 cells with As<sup>3+</sup> and TCDD elicited significant inhibition of TCDD dependent induction of EROD activity over a concentration range from 5  $\mu$ M to 50  $\mu$ M As<sup>3+</sup> (Figure 2A). An excellent correlation was observed when EROD activity was measured both in whole cells as well as in HepG2 cell microsomal preparations (Figure 2B), indicating that the expression of CYP1A1 was dramatically impaired. This was confirmed by Western blot analysis of induced CYP1A1. The pattern of EROD activity correlated with a concentration-dependent reduction in CYP1A1 protein (Figure 3A).

Quantitation of TCDD inducible CYP1A1 mRNA by real time RT-PCR demonstrated that the levels of RNA following TCDD and As<sup>3+</sup> treatment were concordant with reductions seen in CYP1A1 by Western blot analysis. At 0.5  $\mu$ M As<sup>3+</sup>, a concentration that has no detectable effect on cell cycle control, CYP1A1 mRNA induction decreased by 61% of the levels observed with TCDD treatment alone (Figure 3B). At 50  $\mu$ M As<sup>3+</sup> cotreatment a 90% decrease in TCDD induction of CYP1A1 mRNA was observed.

The levels of As<sup>3+</sup> needed to block induction of CYP1A1 were 10 fold lower than those shown to stimulate G2/M arrest, indicating that those events associated with cell cycle control may have limited impact on induction of CYP1A1. However, we cannot exclude the possibility that analysis of cell cycle control in the presence of lower concentration of As<sup>3+</sup> may lie outside the detection limits of flow cytometry. To compensate for this possibility, an experiment was conducted using cultured mouse liver hepatocytes isolated from transgenic *CYP1A1N*<sup>+/-</sup> mice (Galijatovic *et al.*, 2004). When primary hepatocytes are placed in culture, they become quiescent so cell cycle control cannot be credited with alterations in gene expression patterns. Since *CYP1A1N*<sup>+/-</sup> mice express the full length human *CYP1A1* gene, induction of mouse Cyp1a1 and human CYP1A1 can be evaluated simultaneously. As shown in Figure 3C, treatment of hepatocytes with TCDD resulted in a marked induction of Cyp1a1 and CYP1A1. As<sup>3+</sup> cotreatment inhibited in a dose dependent fashion TCDD induction of both mouse Cyp1a1 and human CYP1A1. The inability of lower concentrations of As<sup>3+</sup> to inhibit cell cycle control in HepG2 cells combined with the observations that As<sup>3+</sup> can inhibit induction of CYP1A1 in *CYP1A1N*<sup>+/-</sup> derived primary hepatocytes indicates that the cellular mechanisms initiated by As<sup>3+</sup> on cell cycle control do not influence those events that lead to inhibition of CYP1A1 induction by Ah receptor ligands.

### ***The actions of As<sup>3+</sup> on TCDD-induced transcriptional control of CYP1A1***

The reduction in TCDD enhancement of CYP1A1 by As<sup>3+</sup> might indicate that cellular control of the Ah receptor is a potential target for the actions of As<sup>3+</sup>. When cytosolic preparations from hepalc1c7 cells are incubated with TCDD, the Ah receptor forms a complex with Arnt, generating a transcriptional complex capable of binding to DNA. Ah receptor activation can be demonstrated by receptor binding to XRE sequences, as demonstrated by electromobility gel shift analysis (EMSA). In Figure 4, the addition of TCDD to hepalc1c7 cytosol leads to the identification of an AhR/XRE complex (lane 5). The binding of activated Ah receptor was shown to be specific by the reduction in labeled protein/DNA interactions when the reaction was incubated with excess of cold XRE oligonucleotide (Figure 4, lane 6). Incubation with an inhibitor of Ah receptor ligand binding ( $\alpha$ -naphthoflavone) also demonstrates a specific reduction in binding (Figure 4, lane 7). However, when increasing concentrations of As<sup>3+</sup> were included in the binding reaction, no inhibition of Ah receptor binding to the XRE sequences was noted.

To examine the impact of As<sup>3+</sup> on TCDD induced nuclear accumulation of the Ah receptor, HepG2 cells were treated with TCDD or co-treated with TCDD and As<sup>3+</sup> for 18 hours and nuclear accumulation of the Ah receptor determined by EMSA. The treatment of HepG2 cells with 10 nM TCDD leads to the accumulation of nuclear Ah receptor, which can be specifically identified by disruption of binding to XRE sequences when antibodies to the Ah receptor and Arnt protein are included in the binding reaction (Figure 5B). When HepG2 cells are co-treated with TCDD and varying concentrations of As<sup>3+</sup> for 18 hours, no disruption in the accumulation of nuclear Ah receptor complex is observed (Figure 5A).

To examine directly the impact of As<sup>3+</sup> on TCDD initiated *CYP1A1* transcription, TV101L cells that express the human *CYP1A1* promoter upstream of the firefly luciferase reporter gene were employed. Treatment with TCDD induced luciferase activity 50-fold over untreated cells (Figure

6A). When TV101L cells were co-treated with 10 nM TCDD and varying concentrations of  $\text{As}^{3+}$  for 18 hours,  $\text{As}^{3+}$  had negligible effects on TCDD initiated induction of *CYP1A1*-luciferase activity.

Since activation of the Ah receptor and the initiation of transcription are not influenced by  $\text{As}^{3+}$  exposure, we elected to determine if the rate of *CYP1A1* transcription was altered by measuring the levels of heteronuclear (hnRNA) *CYP1A1* RNA. Quantization of hnRNA is a measurement of the abundance of nuclear transcripts and reflects the rate of RNA synthesis at any steady state level. In this experiment, cells were treated for 1 hour with either TCDD or cotreated with TCDD and  $\text{As}^{3+}$ , and the nuclear *CYP1A1* RNA quantitated by real time RT-PCR using primers that amplify the exon-intron boundary of exon 1 (Hestermann and Brown, 2003). Treatment of HepG2 cells with TCDD induced *CYP1A1* hnRNA after 1 hour treatment (Figure 6B). When cells were cotreated with TCDD at either 0.1 or 0.5  $\mu\text{M}$   $\text{As}^{3+}$ , reduction in the abundance of the hnRNA transcript was noted. The low concentrations of  $\text{As}^{3+}$  were comparable to those that inhibited the induction of mRNA and protein. Thus,  $\text{As}^{3+}$  appears to interfere with the transcriptional processes that promote induction of *CYP1A1*.

Confirmation of the inhibition of transcription on the *CYP1A1* promoter was obtained by the chromatin immunoprecipitation assay (ChIP). HepG2 cells were treated for 1 hr with TCDD or TCDD with either 0.5  $\mu\text{M}$   $\text{As}^{3+}$  or 5  $\mu\text{M}$   $\text{As}^{3+}$ . The pull down was performed with an antibody specific to RNA polymerase II and real-time PCR was performed with primers specific to the proximal promoter of *CYP1A1*. Due to the exponential nature of PCR, the C(t) value difference of 2 between DMSO and TCDD treated cells indicates an approximately 4-fold enrichment of promoter sequences detected in TCDD treated cells (Figure 6C). Cotreatment with 5  $\mu\text{M}$   $\text{As}^{3+}$  raised the C(t) value to almost basal levels indicating a reduction in the amount of pol II recruited to the promoter. These results suggest in conjunction with the hnRNA assay that  $\text{As}^{3+}$  inhibits the recruitment of the basic transcription machinery necessary for TCDD induction of *CYP1A1*.

## Discussion

Our results indicate that  $\text{As}^{3+}$  initiated cell cycle arrest and the inhibition of CYP1A1 induction by TCDD are not associated with a common regulatory event. The disparity in these events can be observed by the very large differences in  $\text{As}^{3+}$  concentrations needed to induce G2/M arrest and the inhibition of TCDD initiated induction CYP1A1 induction. Very clear reductions in the induction of CYP1A1 mRNA and protein are observed at 0.5  $\mu\text{M}$   $\text{As}^{3+}$ , while the early events leading to G2/M arrest are not detectable until 12.5  $\mu\text{M}$   $\text{As}^{3+}$  exposure. One may speculate that  $\text{As}^{3+}$  is capable of initiating cell cycle arrest at very low concentrations but the sensitivity of detecting G2/M arrest exceeds the limits of our techniques. Yet, when we analyzed the potential for cell arrest by monitoring changes in cell cycle regulatory proteins such as the cyclins B1 and D1 (Zhao *et al.*, 2002; Park *et al.*, 2001), p21, cdc25A and cdk1 (Park *et al.*, 2000), no observable changes in these proteins were detected with low concentrations of  $\text{As}^{3+}$  (data not shown). Furthermore, studies conducted in primary hepatocytes would question the role of cell cycle arrest in  $\text{As}^{3+}$  inhibition of TCDD-mediated CYP1A1 induction. Hepatocytes are quiescent cells in the intact liver but are capable of 1-2 progressions through the cell cycle during liver injury. In culture, primary hepatocytes progress through G1 independent of stimulation but arrest in mid-G1 after 42 hours in culture (Talarmin *et al.*, 1999; Loyer *et al.*, 1996). The hepatocytes in our study were cultured for 48 hours prior to treatment allowing for cessation of cycling. Inhibition of TCDD-mediated CYP1A1 induction by  $\text{As}^{3+}$  was still observed and closely resembled the dose-response established in HepG2 cells. Thus, CYP1A1 induction was still dramatically inhibited in a quiescent cell model. These results demonstrate that the actions of  $\text{As}^{3+}$  on blocking CYP1A1 induction by TCDD are initiated through alterations in CYP1A1 transcription and are independent of the regulatory mechanisms initiated by  $\text{As}^{3+}$  induced cell arrest.

The reduction in TCDD-induced CYP1A1-specific EROD activity by  $\text{As}^{3+}$  has been clearly established. Similar results have been observed when cells were cotreated with PAHs and  $\text{As}^{3+}$  (Vernhet *et al.*, 2003; Jacobs *et al.*, 1998; Jacobs *et al.*, 1999; Vakharia *et al.*, 2001a; Vakharia *et al.*, 2001b). It has been postulated that this inhibition is the result of interference by  $\text{As}^{3+}$  with the catalytic potential of CYP1A1, either through reduction in cellular heme pools or by direct binding of  $\text{As}^{3+}$  to CYP1A1. However, changes in cellular heme pools would not lead to the changes in CYP1A1 transcription and the resulting reduction in CYP1A1 as determined by western blot analysis.

The unique ability of  $\text{As}^{3+}$  to bind thiol groups is well established *in vitro* while relevant cellular models of binding are more difficult to determine.  $\text{As}^{3+}$  has been shown to inhibit steroid binding to the glucocorticoid receptor (Stancato *et al.*, 1993; Simons, Jr. *et al.*, 1990) and inactivate the catalytic loop in I $\kappa$ B kinase  $\beta$  subunit (IKK $\beta$ ) thereby reducing NF- $\kappa$ B activity (Kapahi *et al.*, 2000). Members of the cytochrome P450 (CYP) superfamily contain a conserved cysteine residue which serves as the axial ligand for heme iron (Johnson, 2003). However, CYPs contain very few cysteine residues and in the crystal structure of CYP2C5, no other cysteines are found in proximity to the heme binding cysteine. Since coupling to adjacent cysteine residues is a prerequisite for inhibition of protein function by  $\text{As}^{3+}$  and given the evidence presented here on down-regulation of CYP1A1 by a transcriptional mechanism, the inhibition of EROD activity is not the result of arsenic directly associating with CYP1A1.

Recent work has demonstrated a similar pattern of PAH-induced CYP1A1 inhibition by chromium (Wei *et al.*, 2004). This work suggests that heavy metals may be acting in a similar manner at the promoter to inhibit induction of *CYP1A1*. However, chromium and  $\text{As}^{3+}$  show distinct patterns of gene expression alteration.  $\text{As}^{3+}$  alters the expression of a unique set of genes, most notably upregulation of HO-1, metallothionein, and NQO1 while chromium inhibits the expression

of metallothionein and NQO1 (Maier *et al.*, 2000;Andrew *et al.*, 2003;Zheng *et al.*, 2003;Majumder *et al.*, 2003). Chromium's ability to cause DNA-protein cross-links has been suggested as a potential mechanism for HDAC1 sequestration on chromatin surrounding *CYP1A1*, a mechanism that has been proposed to inhibit CYP1A1 transcription. However, As<sup>3+</sup>-induced cross-links and DNA damage have been repeatedly found using primarily very high cytotoxic concentrations (Guillamet *et al.*, 2004;Mouron *et al.*, 2001;Yih and Lee, 2000). Thus, it is doubtful that the low concentrations of As<sup>3+</sup> used in our studies would impact on HDAC1 sequestration.

Our results suggest that the actions of As<sup>3+</sup> leading to inhibition of CYP1A1 induction in HepG2 cells occur following TCDD initiated activation of the Ah receptor and binding of the receptor to DNA. Since the nuclear concentrations of Ah receptor or the binding potential of the Ah receptor/Arnt complex to DNA is not compromised, the reductions in CYP1A1 hnRNA indicate that the rate of transcription initiated by TCDD may be slowed. Because of the low concentrations of As<sup>3+</sup> needed to inhibit TCDD induction of CYP1A1, we would predict that As<sup>3+</sup> is modifying essential regulatory proteins involved in the maintenance of polymerase initiated transcription. In support of this, chromatin immunoprecipitation assays revealed a reduction in pol II recruitment to the *CYP1A1* proximal promoter. Given the specificity of As<sup>3+</sup> inhibition to CYP1A1 this suggests a block of a signaling event involved in the recruitment of pol II to the gene.

Acknowledgments – We thank Dr. Fred Guengerich, Department of Biochemistry, Vanderbilt University, for a sample of the anti-CYP1A1 antibody and Dr. Christopher Bradfield, McArdle Laboratory for Cancer Research, University of Wisconsin, for aliquots of the anti-Ah receptor and anti-Arnt antibodies.

## References

Andrew AS, Warren A J, Barchowsky A, Temple K A, Klei L, Soucy N V, O'Hara K A and Hamilton J W (2003) Genomic and Proteomic Profiling of Responses to Toxic Metals in Human Lung Cells. *Environ Health Perspect* **111**: 825-835.

Chen Y-H and Tukey R H (1996) Protein Kinase C Modulates Regulation of the CYP1A1 Gene by the Ah Receptor. *J Biol Chem* **271**: 26261-26266.

Chiou HY, Huang W I, Su C L, Chang S F, Hsu Y H and Chen C J (1997) Dose-Response Relationship Between Prevalence of Cerebrovascular Disease and Ingested Inorganic Arsenic. *Stroke* **28**: 1717-1723.

Ciolino HP, Daschner P J, Wang T T and Yeh G C (1998) Effect of Curcumin on the Aryl Hydrocarbon Receptor and Cytochrome P450 1A1 in MCF-7 Human Breast Carcinoma Cells. *Biochem Pharmacol* **56**: 197-206.

Elferink CJ, Ge N L and Levine A (2001) Maximal Aryl Hydrocarbon Receptor Activity Depends on an Interaction With the Retinoblastoma Protein. *Mol Pharmacol* **59**: 664-673.

Filippova M and Duerksen-Hughes P J (2003) Inorganic and Dimethylated Arsenic Species Induce Cellular P53. *Chem Res Toxicol* **16**: 423-431.

Galijatovic A, Beaton D, Nguyen N, Chen S, Bonzo J, Johnson R, Maeda S, Karin M, Guengerich F P and Tukey R H (2004) The Human *CYP1A1* Gene Is Regulated in a Developmental and Tissue Specific Fashion in Transgenic Mice. *J Biol Chem*. **279**: 23969-23976.

Guillamet E, Creus A, Ponti J, Sabbioni E, Fortaner S and Marcos R (2004) In Vitro DNA Damage by Arsenic Compounds in a Human Lymphoblastoid Cell Line (TK6) Assessed by the Alkaline Comet Assay. *Mutagenesis* **19**: 129-135.

Hestermann EV and Brown M (2003) Agonist and Chemopreventative Ligands Induce Differential Transcriptional Cofactor Recruitment by Aryl Hydrocarbon Receptor. *Mol Cell Biol* **23**: 7920-7925.

Jacobs J, Roussel R, Roberts M, Marek D, Wood S, Walton H, Dwyer B, Sinclair P and Sinclair J (1998) Effect of Arsenite on Induction of CYP1A and CYP2H in Primary Cultures of Chick Hepatocytes. *Toxicol Appl Pharmacol* **150**: 376-382.

Jacobs JM, Nichols C E, Andrew A S, Marek D E, Wood S G, Sinclair P R, Wrighton S A, Kostrubsky V E and Sinclair J F (1999) Effect of Arsenite on Induction of CYP1A, CYP2B, and CYP3A in Primary Cultures of Rat Hepatocytes. *Toxicol Appl Pharmacol* **157**: 51-59.

Johnson EF (2003) The 2002 Bernard B. Brodie Award Lecture: Deciphering Substrate Recognition by Drug-Metabolizing Cytochromes P450. *Drug Metab Dispos* **31**: 1532-1540.

Kapahi P, Takahashi T, Natoli G, Adams S R, Chen Y, Tsien R Y and Karin M (2000) Inhibition of NF-Kappa B Activation by Arsenite Through Reaction With a Critical Cysteine in the Activation Loop of Ikappa B Kinase. *J Biol Chem* **275**: 36062-36066.

Lee MY, Jung B I, Chung S M, Bae O N, Lee J Y, Park J D, Yang J S, Lee H and Chung J H (2003) Arsenic-Induced Dysfunction in Relaxation of Blood Vessels. *Environ Health Perspect* **111**: 513-517.

Liu L, Trimarchi J R, Navarro P, Blasco M A and Keefe D L (2003) Oxidative Stress Contributes to Arsenic-Induced Telomere Attrition, Chromosome Instability, and Apoptosis. *J Biol Chem* **278**: 31998-32004.

Loyer P, Cariou S, Glaise D, Bilodeau M, Baffet G and Guguen-Guillouzo C (1996) Growth Factor Dependence of Progression Through G1 and S Phases of Adult Rat Hepatocytes in Vitro. Evidence of a Mitogen Restriction Point in Mid-Late G1. *J Biol Chem* **271**: 11484-11492.

Maier A, Dalton T P and Puga A (2000) Disruption of Dioxin-Inducible Phase I and Phase II Gene Expression Patterns by Cadmium, Chromium, and Arsenic. *Mol Carcinog* **28**: 225-235.

Majumder S, Ghoshal K, Summers D, Bai S, Datta J and Jacob S T (2003) Chromium(VI) Down-Regulates Heavy Metal-Induced Metallothionein Gene Transcription by Modifying Transactivation Potential of the Key Transcription Factor, Metal-Responsive Transcription Factor 1. *J Biol Chem* **278**: 26216-26226.

Mosmann T (1983) Rapid Colorimetric Assay for Cellular Growth and Survival: Application to Proliferation and Cytotoxicity Assays. *J Immunol Methods* **65**: 55-63.

Mouron SA, Golijow C D and Dulout F N (2001) DNA Damage by Cadmium and Arsenic Salts Assessed by the Single Cell Gel Electrophoresis Assay. *Mutat Res* **498**: 47-55.

Park JW, Choi Y J, Jang M A, Baek S H, Lim J H, Passaniti T and Kwon T K (2001) Arsenic Trioxide Induces G2/M Growth Arrest and Apoptosis After Caspase-3 Activation and Bcl-2 Phosphorylation in Promonocytic U937 Cells. *Biochem Biophys Res Commun* **286**: 726-734.

Park WH, Seol J G, Kim E S, Hyun J M, Jung C W, Lee C C, Kim B K and Lee Y Y (2000) Arsenic Trioxide-Mediated Growth Inhibition in MC/CAR Myeloma Cells Via Cell Cycle Arrest in

Association With Induction of Cyclin-Dependent Kinase Inhibitor, P21, and Apoptosis. *Cancer Res* **60**: 3065-3071.

Pfaffl MW (2001) A New Mathematical Model for Relative Quantification in Real-Time RT-PCR. *Nucleic Acids Res* **29**: pp e45.

Postlind H, Vu T P, Tukey R H and Quattrochi L C (1993) Response of Human *CYP1A*-Luciferase Plasmids to 2,3,7,8- Tetrachlorodibenzo-*p*-Dioxin and Polycyclic Aromatic Hydrocarbons. *Toxicol Appl Pharmacol* **118**: 255-262.

Santini RP, Myrand S, Elferink C and Reiners J J, Jr. (2001) Regulation of Cyp1a1 Induction by Dioxin As a Function of Cell Cycle Phase. *J Pharmacol Exp Ther* **299**: 718-728.

Schwerdtle T, Walter I, Mackiw I and Hartwig A (2003) Induction of Oxidative DNA Damage by Arsenite and Its Trivalent and Pentavalent Methylated Metabolites in Cultured Human Cells and Isolated DNA. *Carcinogenesis* **24**: 967-974.

Simons SS, Jr., Chakraborti P K and Cavanaugh A H (1990) Arsenite and Cadmium(II) As Probes of Glucocorticoid Receptor Structure and Function. *J Biol Chem* **265**: 1938-1945.

Smith AH, Hopenhayn-Rich C, Bates M N, Goeden H M, Hertz-Picciotto I, Duggan H M, Wood R, Kosnett M J and Smith M T (1992) Cancer Risks From Arsenic in Drinking Water. *Environ Health Perspect* **97**: 259-267.

Stancato LF, Hutchison K A, Chakraborti P K, Simons S S, Jr. and Pratt W B (1993) Differential Effects of the Reversible Thiol-Reactive Agents Arsenite and Methyl Methanethiosulfonate on Steroid Binding by the Glucocorticoid Receptor. *Biochemistry* **32**: 3729-3736.

Talarmin H, Rescan C, Cariou S, Glaise D, Zanninelli G, Bilodeau M, Loyer P, Guguen-Guillouzo C and Baffet G (1999) The Mitogen-Activated Protein Kinase Kinase/Extracellular Signal-Regulated Kinase Cascade Activation Is a Key Signalling Pathway Involved in the Regulation of G(1) Phase Progression in Proliferating Hepatocytes. *Mol Cell Biol* **19**: 6003-6011.

Tchounwou PB, Patlolla A K and Centeno J A (2003) Carcinogenic and Systemic Health Effects Associated With Arsenic Exposure--a Critical Review. *Toxicol Pathol* **31**: 575-588.

Vakharia DD, Liu N, Pause R, Fasco M, Bessette E, Zhang Q Y and Kaminsky L S (2001) Polycyclic Aromatic Hydrocarbon/Metal Mixtures: Effect on PAH Induction of CYP1A1 in Human HEPG2 Cells. *Drug Metab Dispos* **29**: 999-1006.

Vernhet L, Allain N, Le Vee M, Morel F, Guillouzo A and Fardel O (2003) Blockage of Multidrug Resistance-Associated Proteins Potentiates the Inhibitory Effects of Arsenic Trioxide on CYP1A1 Induction by Polycyclic Aromatic Hydrocarbons. *J Pharmacol Exp Ther* **304**: 145-155.

Wei YD, Tepperman K, Huang M Y, Sartor M A and Puga A (2004) Chromium Inhibits Transcription From Polycyclic Aromatic Hydrocarbon-Inducible Promoters by Blocking the Release of Histone Deacetylase and Preventing the Binding of P300 to Chromatin. *J Biol Chem* **279**: 4110-4119.

Yih LH and Lee T C (2000) Arsenite Induces P53 Accumulation Through an ATM-Dependent Pathway in Human Fibroblasts. *Cancer Res* **60**: 6346-6352.

Yueh MF, Huang Y H, Hiller A, Chen S J, Nguyen N and Tukey R H (2003) Involvement of the Xenobiotic Response Element (XRE) in Ah Receptor-Mediated Induction of Human UDP-Glucuronosyltransferase 1A1. *Journal of Biological Chemistry* **278**: 15001-15006.

Zheng XH, Watts G S, Vaught S and Gandolfi A J (2003) Low-Level Arsenite Induced Gene Expression in HEK293 Cells. *Toxicology* **187**: 39-48.

Footnotes. This work was supported by Superfund Basic Research Program grant ES10337 from the United States Public Health Service.

† Present Address.

Biochemical and Investigative Toxicology

Merck & Co. Inc.

WP45A-201

770 Sumneytown Pike

West Point, PA 19486

## FIGURE LEGENDS

**Figure 1.** *Cell viability, apoptosis and cell cycle arrest following As<sup>3+</sup> exposure.* A) HepG2 and TV101L cells were treated with 10 nM TCDD and indicated concentrations of As<sup>3+</sup> for 18 hours. Cell viability was measured using the MTT assay and expressed as percent viability compared to TCDD treated cells. Experiments were performed in triplicate. Significant decrease from viability of TCDD-treated cells is indicated (\*, P≤0.05). B) HepG2 cells were treated with 10 nM TCDD and indicated concentrations of As<sup>3+</sup> for 18 hours. Twenty µg of whole cell extract was used for Western blot analysis of PARP-1 cleavage. Intact PARP-1 (116 kD) and cleaved PARP-1 (85 kD) are indicated. Extracts from BPDE-2 treated cells was used as a positive control for cleavage. Blots were re-washed and exposed to anti-β-actin for loading control. C). HepG2 cells were treated with 10 nM TCDD and various concentrations of As<sup>3+</sup> for 18 hours before fixation. Ten thousand PI stained cells were acquired on a FACS Calibur flow cytometer, and the percent of cells in G2/M as a result of As<sup>3+</sup> treatment is shown. Cells were treated with TCDD or TCDD and increasing As<sup>3+</sup> concentrations. Data shown indicate the percent of the total cells counted that were in G2/M phase after As<sup>3+</sup> treatment and are representative of three independent FACS analyses.

**Figure 2.** *EROD activity as a function of As<sup>3+</sup> treatment.* A) HepG2 cells were treated with 10 nM TCDD and increasing concentrations of As<sup>3+</sup> for 18 hours and cellular EROD activity measured as outlined in Materials and Methods. B) HepG2 cells were treated with 10 nM TCDD and increasing concentrations of As<sup>3+</sup> for 18 hours and microsomes were collected. Microsomal EROD activity was determined using 20 µg protein in reaction mixture as outlined in Materials and Methods. Significant decreases in EROD activity from TCDD treatment are indicated (\*, P≤0.05).

**Figure 3.** *CYP1A1* protein and mRNA expression decreases with  $As^{3+}$  treatment. **A)** HepG2 cells were treated with 10 nM TCDD and various concentrations of  $As^{3+}$  for 18 hours at which time microsomes were collected. Ten  $\mu$ g of microsomes were used for western blot analysis. **B)** Real-time RT-PCR results were normalized to GAPDH and expressed as % induction of TCDD treated cells. Significant decreases in mRNA expression from TCDD treatment are indicated (\*,  $P \leq 0.05$ ). **C)** Primary hepatocytes were isolated from *CYP1A1*<sup>+/+</sup> transgenic mice and exposed in culture to TCDD and various  $As^{3+}$  concentrations. Whole cell lysates were collected and 20  $\mu$ g of protein used for Western blot detection using the human CYP1A1 antibody that is cross-reactive with mouse Cyp1a1. Whole cell extracts from TCDD treated hepalc1c7 cells were used as a positive control for mouse Cyp1a1 and TCDD treated HepG2 whole cell extracts were used as a human CYP1A1 positive control.

**Figure 4.** *Activation of Ah receptor is unaffected by the presence of  $As^{3+}$ .* Cytosolic extracts (50  $\mu$ g) from untreated Hepalclc7 cells were incubated with 20 nM TCDD and indicated  $As^{3+}$  concentrations for 20 hours at 4°C. Gel shift was performed as described. Control reactions are as follows: free probe (*lane 1*), water (*lane 2*), DMSO (*lane 3*), 5  $\mu$ M  $As^{3+}$  (*lane 4*), 20 nM TCDD (*lane 5*), 20nM TCDD and 200X unlabelled XRE (*lane 6*), and 20 nM TCDD + 1  $\mu$ M  $\beta$ -naphthoflavone (*lane 7*). Co-incubation of TCDD and  $As^{3+}$  are indicated (*lanes 8-12*). Activated Ah receptor (AhR)/Arnt heterodimer is indicated. Gel shift is representative of three independent experiments.

**Figure 5.** *Ah receptor nuclear translocation and DNA binding activity is unchanged by  $As^{3+}$  treatment.* **A)** Nuclear protein was prepared from HepG2 cells treated for 18 hours with 10 nM TCDD and increasing concentrations of  $As^{3+}$  as described in Materials and Methods. Ten  $\mu$ g of

nuclear protein was incubated with  $^{32}\text{P}$ -XRE ( $5 \times 10^5$  cpm). Controls are as indicated: free probe (*lane 1*), DMSO treatment (*lane 2*),  $5 \mu\text{M}$   $\text{As}^{3+}$  treatment (*lane 3*),  $10 \text{ nM}$  TCDD treatment (*lane 4*), and TCDD treatment incubated with 200X unlabelled XRE as a specific competitor control (*lane 5*). Shifts of TCDD and  $\text{As}^{3+}$  cotreatments are indicated (*lanes 6-10*). Gel shown is representative of three independent shifts. B) Supershift analysis was performed using  $10 \text{ nM}$  TCDD and  $10 \text{ nM}$  TCDD with  $25 \mu\text{M}$   $\text{As}^{3+}$  nuclear protein preparations. Activated AhR/Arnt binding complex was competed with 200X unlabelled XRE (*lanes 2 and 7*). Specificity of binding was determined by incubation with  $200 \text{ ng}$  anti-Ah receptor (*lanes 4 and 9*) and  $100 \text{ ng}$  anti-Arnt (*lanes 5 and 10*) antibodies. Nonspecific antibody binding was determined using excess anti-UGT (*lanes 6 and 11*).

**Figure 6. Transcriptional control of CYP1A1.** A) TV101L cells were co-treated for 18 hours with  $10 \text{ nM}$  TCDD and increasing concentrations of  $\text{As}^{3+}$ . Results are displayed as RLU per  $\mu\text{g}$  cellular protein. All experiments were done in triplicate and a significant increase from  $10 \text{ nM}$  TCDD treatment is indicated (\*,  $P \leq 0.05$ ). B) HepG2 cells were treated for 1 hour with TCDD or TCDD and  $\text{As}^{3+}$ . RNA was collected as described in Materials and Methods. Quantitative RT-PCR results using primers specific for CYP1A1 hnRNA were normalized to GAPDH and expressed as % induction of TCDD treated cells. C) ChIP assay was performed with HepG2 cells treated for 1 hour with TCDD or TCDD and  $\text{As}^{3+}$ . Cells were crosslinked and incubated with antibody specific for Pol II. Recovered DNA was subjected to PCR with primers specific to the proximal promoter of CYP1A1. Results are shown as raw C(t) value and are representative of three independent pull-down experiments.

**Figure 1**

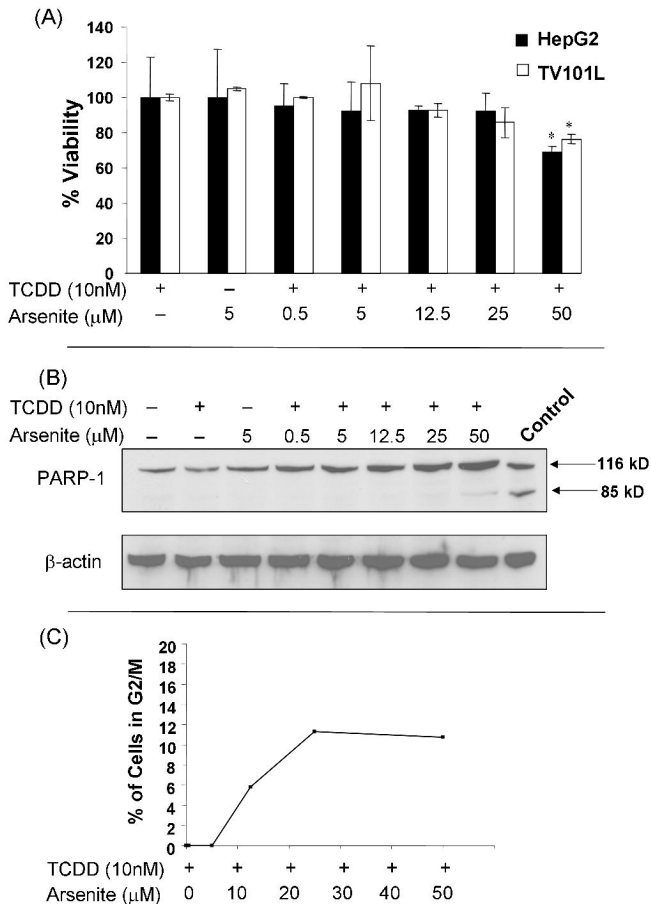


**FIGURE 2.**

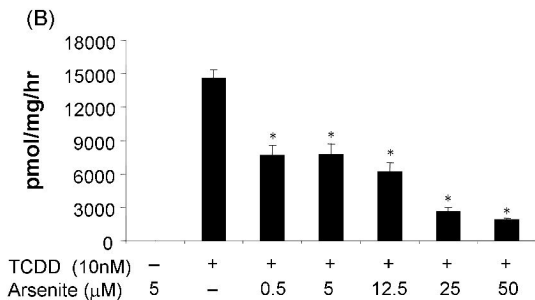
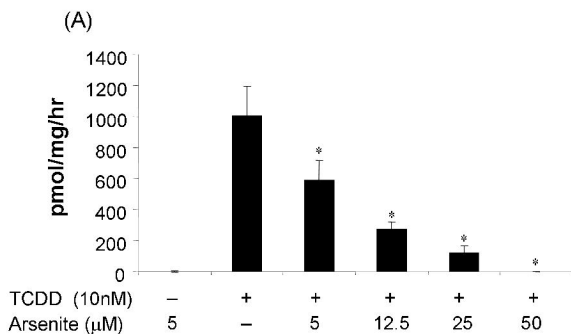


**FIGURE 3.**

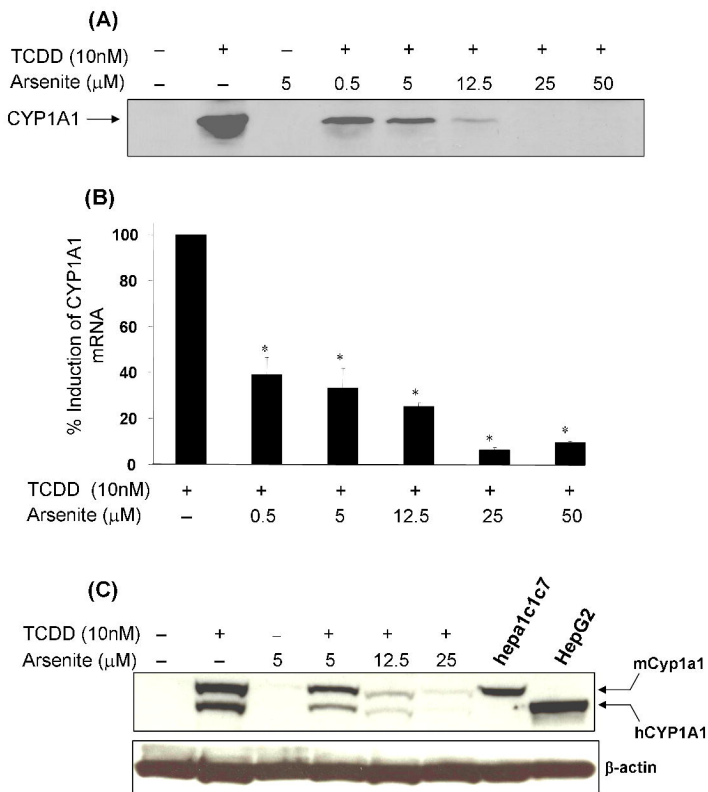


**FIGURE 4.**

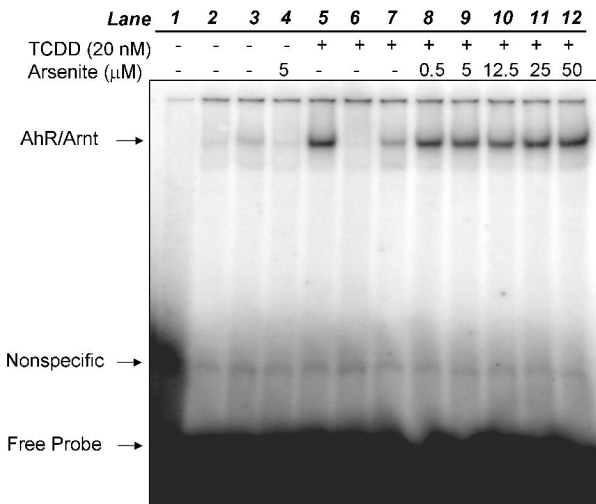
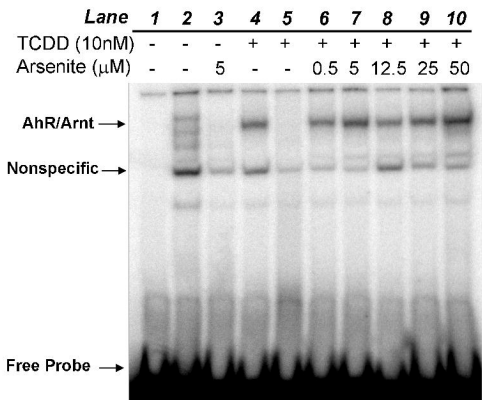
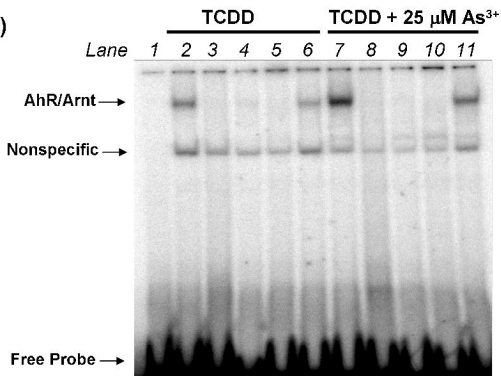


FIGURE 5.

(A)

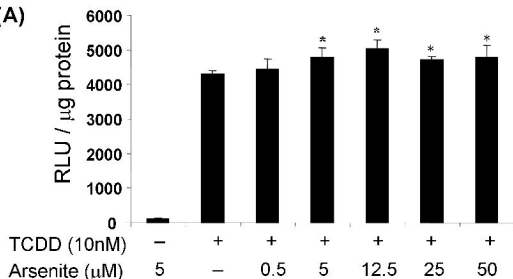


(B)

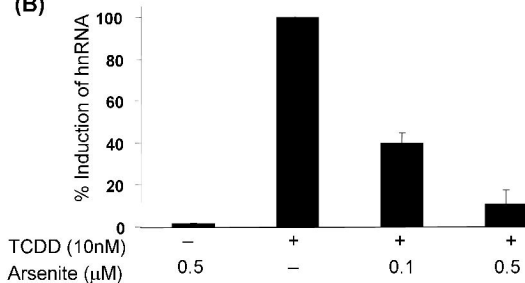


**FIGURE 6.**

**(A)**



**(B)**



**(C)**

